

# SLIDING SYSTEM PREDICTING LARGE PERMANENT CO-SEISMIC MOVEMENTS OF SLOPES

CONSTANTINE A. STAMATOPOULOS

*Kotzias-Stamatopoulos Co. Ltd., 5 Isavron St., Athens 114-71, Greece*

## SUMMARY

The sliding-block model is used widely for the prediction of permanent co-seismic displacements of slopes and earth structures. This model assumes motion in an inclined plane but does not consider the decrease in inclination of the sliding soil mass as a result of its downward motion, which is the usual state in the field. For the investigation of the above effect, this paper considers the dynamic motion of a variant sliding system; a perfectly flexible chain sliding along planes with gradually gentler inclinations. The governing equation of motion of the new model is approximately derived and solved for a number of earthquakes. The cases of ground slips where the permanent displacement of the new model differs considerably from that of the sliding-block model are detected and an improved method predicting permanent seismic deformations is proposed.

KEY WORDS: seismic ground deformations; ground slips; slopes; sliding-block; sliding-chain; critical acceleration

## 1. INTRODUCTION

In the field of Geotechnical Earthquake Engineering there are renewed calls for design approaches and evaluative techniques based upon permanent displacements.<sup>1</sup> Evaluations based on the dynamic factor of safety calculated from loads, or on the danger of liquefaction alone, depend on simplified assumptions that can lead to excessively conservative and costly design. Simplified models predicting seismic ground displacements are less accurate than methods using finite-elements, but have the advantage of readily available solutions and simplicity that makes them usable by practising engineers. In addition, application of sophisticated finite-element models requires accurate field data which are often sparse and incomplete. Thus, further development of simplified models, such as the one presented in this paper, is appropriate.

Permanent shear ground seismic movement can be separated into at least two stages.<sup>2</sup> In the first stage, which is co-seismic, gravity in combination with transient seismic forces, may bring about temporary instability and permanent displacements on a failure surface. The second stage, which is post-seismic, follows immediately after the earthquake and causes large movement if, as a result of the first stage, the strength on the slip surface is reduced to a residual value which is less than that required to maintain static equilibrium. Driving forces during the second stage will be due purely to gravity, and motion will stop primarily due to changes of geometry towards a more stable configuration.

The sliding-block model,<sup>3</sup> shown in Figure 1, forms the basis of simple models predicting permanent co-seismic shear displacements of soils. In this model, critical acceleration is defined as the horizontal acceleration that causes the shear stress to become equal to the shear strength at the base of a block-on-an-inclined-plane. When the applied acceleration is larger than the critical acceleration, the block slides. The total displacement is obtained by the addition of the slips where relative motion develops. This model has been used for the estimation of permanent seismic deformations of natural slopes without considerable earthquake-induced loss of strength,<sup>2</sup> in earth dams,<sup>4,5</sup> rockfill dams,<sup>6</sup> gravity walls retaining dry soil<sup>7</sup> and shallow foundations on dry soil.<sup>8</sup> The solutions giving the distance moved by the sliding-block are used for the prediction of permanent seismic movement of these problems by replacing the maximum applied

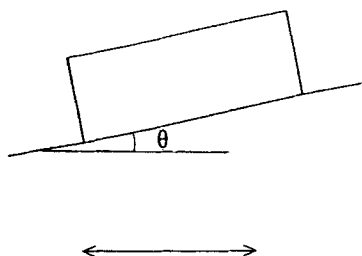


Figure 1. The sliding-block model: a block sliding on an inclined plane by a horizontal excitation

acceleration and critical acceleration of the block with those of the potential sliding mass under consideration. The critical acceleration of the sliding mass is estimated by stability or limit-plasticity analyses and the maximum applied acceleration is often obtained by dynamic analyses.

The sliding-block model is generally successful in estimating small ground deformations without earthquake-induced loss of strength.<sup>1</sup> However, when the ground deformations are large, it is not accurate primarily because of (a) earthquake-induced loss of strength in saturated soils and (b) changes of geometry of the soil mass towards a gentler inclination. Various efforts have been made to incorporate the first effect in the estimation of co-seismic deformations taking into account loss of shear strength<sup>5,9</sup> and/or pore-pressure build-up.<sup>4,10</sup> In this paper the mathematical derivations are for constant strength, but ways to take into account loss of strength are discussed in Section 5. The second effect is discussed in detail; it is the usual state in the field, and is caused by the law of physical equilibrium where masses move towards a more stable configuration. It reduces seismic deformations and has been considered for the prediction of both co-seismic<sup>11,12</sup> and post-seismic<sup>13,14,2</sup> ground displacements.

To incorporate the decrease in inclination of the sliding mass in the estimation of co-seismic displacements the present work considers the earthquake-induced downward movement of a perfectly flexible but inextensible chain sliding along 'n' planes with gradually smaller inclinations. Similarly to Timoshenko and Young,<sup>15</sup> it is assumed that density and cross-section along the chain are constant. To simplify the solution, the part of the chain that changes inclination is assumed to have uniform height, while the height of the other parts of the chain is arbitrary (Figure 2).

The governing equation of motion of the new sliding system is approximately derived and solved for a number of earthquakes. The cases of ground slips where the permanent displacement of the new sliding system differs considerably from that of the block-on-an-inclined-plane system are detected and an improved method predicting permanent seismic deformations is proposed.

## 2. GOVERNING EQUATION OF THE NEW MODEL

### 2.1. The model

In the new model of Figure 2, a chain slides in 'n' planes ('1' to 'n'), where plane '1' has the steepest inclination, plane '2' the smallest and planes '3' to 'n' lie between the planes '2' and '1' with successively increasing inclinations. The chain is part of a torus with constant cross-section and density. Similarly to the sliding-block model, the mass slides uniformly with constant velocity along the trajectory. The parameters that define the geometry of the model of Figure 2 are the angles of inclination with the horizontal of the planes,  $\theta_1, \theta_2, \dots, \theta_n$ , the initial cross-sectional areas of the chain on the first and second sliding plane,  $A_{10}$  and  $A_{20}$ , the initial contact lengths  $b_{10}, b_{20}, \dots, b_{n0}$ , the height of the part that changes inclination,  $h$ , and the distance moved along the trajectory,  $u$ . It can be noted that the initial cross-sectional areas,  $A_{30}, \dots, A_{n-1,0}, A_{n,0}$ , are equal to  $h \times b_{30}, \dots, h \times b_{n-1,0}, h \times b_{n0}$ , respectively. The width of the chain in the direction not present in the cross-section of Figure 2 is denoted as 'w'.

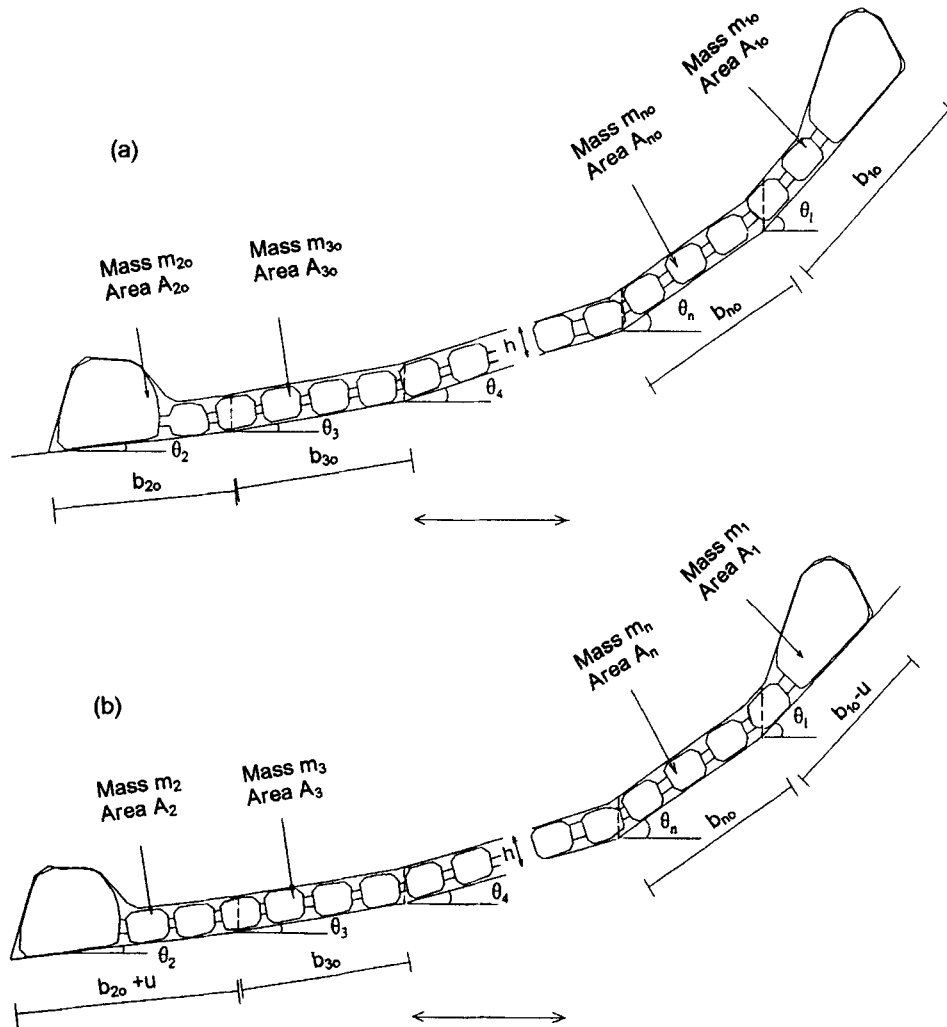


Figure 2. New model: a chain with uniform cross-section sliding in 'n' planes with gradually smaller inclinations by a horizontal excitation. The part that changes inclination has constant height. (a) Initial position, (b) position when the displacement is  $u$

The system considered consists of small rigid bodies connected together by frictionless hinges that do not produce work.<sup>15</sup> In this system, similarly to the sliding-block model, work is done only along the base, against the base resistance. In soils, the inclinations being different, soil will have to shear internally. Therefore, this is a simplified approach, possibly giving displacement larger than the expected.

According to the theory of soil mechanics,<sup>16</sup> both friction and cohesion components of resisting forces are taken to act on the surface of sliding. Analysis is in terms of effective stresses, and pore pressures are considered at the base of the sliding system. Friction, cohesion and pore pressure can take different values in each sliding plane, but are assumed constant as the system slides. Even though analysis is in terms of effective stresses, the equations derived can also be used in analysis based on total stresses, if the undrained shear strength of the soil is used in the place of cohesion, and frictional resistance and pore pressure are taken zero.

## 2.2. Correlations between masses and movements

Depending on the different directions of movement, the sliding chain is divided in 'n' parts, with masses  $m_1, m_2, \dots, m_n$ , as shown in Figure 2. The masses  $m_1$  and  $m_2$  change as a function of the distance moved,

because part of the mass changes inclination of movement, and after parting from  $m_1$  it is added to  $m_2$ . The other masses  $m_3, \dots, m_n$  do not change. The masses  $m_1$  and  $m_2$  are given by

$$m_1 = \rho w(A_{10} - hu) \quad (1a)$$

$$m_2 = \rho w(A_{20} + hu) \quad (1b)$$

where  $u$  is the downward distance moved along the trajectory,  $\rho$  is the average density of the chain and the other parameters were defined previously. The contact lengths  $b_3, \dots, b_n$  do not change. The contact lengths  $b_1$  and  $b_2$  can be expressed in terms of their initial values,  $b_{10}$  and  $b_{20}$ , as

$$b_1 = b_{10} - u \quad (2a)$$

$$b_2 = b_{20} + u \quad (2b)$$

The horizontal coordinate of the center of mass of a system of particles is given as the summation of the mass of each particle times its horizontal coordinate, divided by the total mass of the system.<sup>15</sup> Thus, the incremental horizontal distance that the centre of mass of the sliding chain moves,  $dS$ , equals the summation of the mass of each individual part sliding at inclination ' $i$ ',  $m_i$ , times the incremental horizontal distance that it moves,  $\{du \cos \theta_i\}$ , divided by the total mass:

$$dS = \frac{\sum_{i=1}^n (m_i du \cos \theta_i)}{\sum_{i=1}^n m_i} = \frac{\sum_{i=1}^n (A_{i0} \cos \theta_i) + uh(\cos \theta_2 - \cos \theta_1)}{A_t} du \quad (3a)$$

where  $A_t$  is total area of the sliding chain in the cross-section shown in Figure 2. Solution of the above equation for the distance  $u$ , in Appendix I, gives

$$u = \frac{2SA_t / \sum_{i=1}^n (A_{i0} \cos \theta_i)}{1 + \left(1 + \frac{2Sh(\cos \theta_2 - \cos \theta_1)A_t}{(\sum_{i=1}^n A_{i0} \cos \theta_i)^2}\right)^{0.5}} \quad (3b)$$

### 2.3. Critical acceleration

Critical acceleration,  $a_c$ , is the limiting horizontal acceleration that when applied on a body causes movement. Figure 3 gives the forces that act on the part of the chain of Figure 2 on level with inclination ' $i$ ',

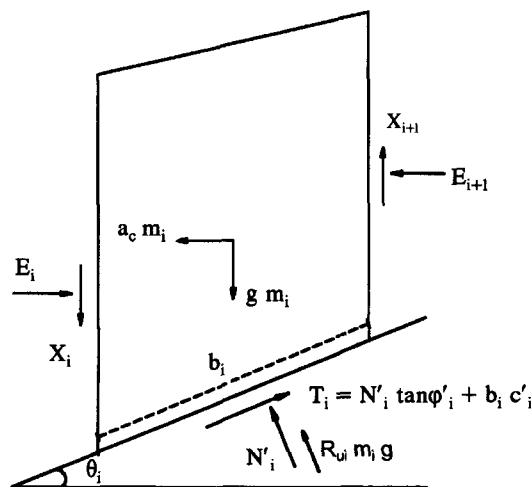


Figure 3. Force diagram of the part of the chain of Figure 2 sliding at plane ' $i$ '

when the critical acceleration acts on the sliding chain and water pressure exists at the base of the system, in terms of effective stresses. These forces are:

- (1) the force of gravity, given by the acceleration of gravity times the mass,  $\{gm_i\}$ ;
- (2) the reaction force between the sliding mass and the plane, in terms of effective stresses,  $N'_i$ ;
- (3) the resistance to motion,  $T_i$ , that equals  $\{c'_iwb_i + N'_i \tan \varphi'_i\}$ , where  $c'_i$  and  $\varphi'_i$  are the effective cohesion and frictional resistance on the surface of sliding with inclination 'i',
- (4) force due to pore pressure at the base, expressed in terms of the weight, as  $\{R_{ui}gm_i\}$ , where  $R_u$  is the pore pressure ratio, defined as the ratio of pore pressure by total vertical stress,
- (5) the change in horizontal and vertical forces between the adjacent parts,  $DE_i$  and  $DX_i$ , that equal to  $\{E_{i+1} - E_i\}$  and  $\{X_{i+1} - X_i\}$  respectively, and
- (6) the inertia force as a result of the critical acceleration,  $\{a_c m_i\}$ .

This problem, where the critical acceleration acts on a mass sliding in 'n' planes with gradually gentler inclinations is considered by Sarma.<sup>17</sup> Compared to Reference [17], in the present formulation the length  $b_i$  is defined differently, along the trajectory instead of horizontally. Equilibrium for each slice with a base with inclination 'i', and the whole mass, is given in Reference 17:

$$a_c m_i = gm_i \left( \tan(\varphi'_i - \theta_i) - R_{ui} \sin \varphi'_i \sec \theta_i / \cos(\varphi'_i - \theta_i) \right) + c'_i w b_i \cos \varphi'_i / \cos(\varphi'_i - \theta_i) - DE_i - DX_i \tan(\varphi'_i - \theta_i) \quad (4a)$$

$$a_c m_t = g \sum_{i=1}^n \left( m_i (\tan(\varphi'_i - \theta_i) - R_{ui} \sin \varphi'_i \sec \theta_i / \cos(\varphi'_i - \theta_i)) \right) + w \sum_{i=1}^n \left( c'_i b_i \cos \varphi'_i / \cos(\varphi'_i - \theta_i) \right) - \sum_{i=1}^n \left( DX_i \tan(\varphi'_i - \theta_i) \right) \quad (4b)$$

when adding equations (4a) to get equation (4b), the internal forces  $DE_i$  cancel, because their sum equals zero.<sup>17</sup> Separation of the initial values of the masses and lengths of each part of the chain from those when the distance moved along the trajectory is  $u$ , based on equations (1) and (2), gives

$$\begin{aligned} w \rho a_c A_t = w \rho g \sum_{i=1}^n & \left( A_{i0} (\tan(\varphi'_i - \theta_i) - R_{ui} \sin \varphi'_i \sec \theta_i / \cos(\varphi'_i - \theta_i)) \right) \\ & + w \rho g u h \left( -\tan(\varphi'_1 - \theta_1) + \tan(\varphi'_2 - \theta_2) + R_{u1} \sin \varphi'_1 \sec \theta_1 / \cos(\varphi'_1 - \theta_1) \right. \\ & \left. - R_{u2} \sin \varphi'_2 \sec \theta_2 / \cos(\varphi'_2 - \theta_2) \right) + w \sum_{i=1}^n \left( c'_i b_{i0} \cos \varphi'_i / \cos(\varphi'_i - \theta_i) \right) \\ & - w u \left( c'_1 \cos \varphi'_1 / \cos(\varphi'_1 - \theta_1) - c'_2 \cos \varphi'_2 / \cos(\varphi'_2 - \theta_2) \right) - \sum_{i=1}^n \left( DX_i \tan(\varphi'_i - \theta_i) \right) \end{aligned} \quad (4c)$$

Equilibrium of the initial configuration of the sliding chain (i.e. for  $u = 0$ ) can be expressed, from equation (4c), as

$$\begin{aligned} w \rho a_{c0} A_t = w \rho g \sum_{i=1}^n & \left( A_{i0} (\tan(\varphi'_i - \theta_i) - R_{ui} \sin \varphi'_i \sec \theta_i / \cos(\varphi'_i - \theta_i)) \right) \\ & + w \sum_{i=1}^n \left( c'_i b_{i0} \cos \varphi'_i / \cos(\varphi'_i - \theta_i) \right) - \sum_{i=1}^n \left( DX_{i0} \tan(\varphi'_i - \theta_i) \right) \end{aligned} \quad (5)$$

where  $a_{c0}$  is the critical acceleration corresponding to the initial configuration, and the subscript '0' indicates values corresponding to the initial configuration. It is assumed that internal forces are not affected by

changes in geometry (i.e.  $DX_{i0} = DX_i$ ). Then, according to equation (5), equation (4c) can be expressed as

$$wpa_c A_t = wpa_{c0} A_t + wpguhK \quad (4d)$$

or

$$a_c = a_{c0} + guhK/A_t \quad (4e)$$

where

$$\begin{aligned} K = & \tan(\varphi'_2 - \theta_2) - \tan(\varphi'_1 - \theta_1) \\ & + R_{u1} \sin \varphi'_1 \sec \theta_1 / \cos(\varphi'_1 - \theta_1) - R_{u2} \sin \varphi'_2 \sec \theta_2 / \cos(\varphi'_2 - \theta_2) \\ & + c'_2 \cos \varphi'_2 / (\gamma h \cos(\varphi'_2 - \theta_2)) - c'_1 \cos \varphi'_1 / (\gamma h \cos(\varphi'_1 - \theta_1)) \end{aligned} \quad (6a)$$

where  $\gamma$  is the unit weight, equal to  $\{\rho g\}$ .

In equation (4e), as the chain slides a distance  $u$ , the term

$$\left\{ \left( guh/A_t \right) \left( \tan(\varphi'_2 - \theta_2) - \tan(\varphi'_1 - \theta_1) + R_{u1} \sin \varphi'_1 \sec \theta_1 / \cos(\varphi'_1 - \theta_1) - R_{u2} \sin \varphi'_2 \sec \theta_2 / \cos(\varphi'_2 - \theta_2) \right) \right\}$$

represents the incremental increase of the critical acceleration as a result of the change in inclination of the weight, while the term

$$\left\{ \left( guh/A_t \right) \left( c'_2 \cos \varphi'_2 / (\gamma h \cos(\varphi'_2 - \theta_2)) - c'_1 \cos \varphi'_1 / (\gamma h \cos(\varphi'_1 - \theta_1)) \right) \right\}$$

represents the incremental increase of the critical acceleration as a result of the change in the direction of the cohesional resistance with respect to the horizontal.

#### 2.4. Parameters $\kappa_1, \kappa_2$

For brevity, the following symbols will be introduced:

$$\kappa_1 = gK \frac{h}{\sum_{i=1}^n (A_{i0} \cos \theta_i)} \quad (6b)$$

$$\kappa_2 = \frac{2h(\cos \theta_2 - \cos \theta_1) A_t}{(\sum_{i=1}^n A_{i0} \cos \theta_i)^2} \quad (6c)$$

where the factor  $K$  is given by equation (6a).

In the international system of units the parameter  $\kappa_1$  has units ( $1/s^2$ ), and the parameter  $\kappa_2$  ( $1/m$ ). Using the parameters  $\kappa_1$  and  $\kappa_2$ , and equation (3b) relating the distances  $u$  and  $S$ , equation (4e) can be expressed as

$$a_c = a_{c0} + \frac{2S\kappa_1}{1 + (1 + S\kappa_2)^{0.5}} \quad (4f)$$

#### 2.5. Permanent displacements

The horizontal permanent displacement of the center of mass of the sliding chain,  $S$ , when a horizontal dynamic excitation  $a(t)$  is applied on the underlying planes can be obtained, according to Newton's second law of motion, by double integration of

$$\frac{d^2 S}{dt^2} = a(t) - a_c = a(t) - a_{c0} - \frac{2S\kappa_1}{1 + (1 + S\kappa_2)^{0.5}} \quad \text{for } dS/dt > 0 \quad (7)$$

where  $t$  represents time (and thus  $dS/dt$  is the relative velocity and  $d^2 S/dt^2$  is the relative acceleration). Displacement accumulates only when the chain slides downwards (i.e.  $dS/dt > 0$ ), because only then the resistance between the chain and the plane(s) is mobilized.

### 3. TYPICAL VALUES AND APPROXIMATION OF EQUATION (7)

#### 3.1. Computer program and excitations that are applied

A computer program was written that solves numerically equation (7) using Euler's method.<sup>18</sup> The initial displacement and velocity are taken equal to zero. Input for this program includes the values of the coefficients  $\kappa_1$  and  $\kappa_2$ , the maximum applied acceleration  $a_m$ , and the acceleration ratio  $a_{c0}/a_m$ . The shape of the applied excitation  $a(t)$  can be rectangular, triangular sinusoidal or arbitrary. For harmonic excitations, the period and number of cycles of loading/unloading and the shape are specified. For arbitrary excitations, points defining the accelerogram are given.

In the present work, in addition to harmonic excitations, the following accelerograms are applied:

- (a) El-Centro (California, U.S.A.), 18/5/1940, component NS,  $M$  (= earthquake magnitude in the Richter scale) = 6.5,  $R$  (= distance from the epicenter) = 5 km,  $a_m$  (= maximum acceleration) = 0.35  $g$ ,  $T_f$  (= fundamental period) = 0.6 s.
- (b) San Fernando-Avenue of Stars (California, U.S.A.), 1971, component EW,  $M$  = 6.5,  $R$  = 40 km,  $a_m$  = 0.15  $g$ ,  $T_f$  = 0.15 s.
- (c) Kalamata (Greece), 13/9/1986,  $M$  = 5.75,  $R$  = 9 km, Municipality Building, component longitudinal and transverse; long.:  $a_m$  = 0.24  $g$ ,  $T_f$  = 0.35 s, trans.:  $a_m$  = 0.23  $g$ ,  $T_f$  = 0.3 s.
- (d) Gazli (USSR), 17/5/1976,  $M$  = 7.3,  $a_m$  = 0.70  $g$ ,  $T_f$  = 0.1 s,

It can be observed that in these accelerograms the maximum acceleration takes values between 0.15 and 0.70 times the acceleration of gravity and their fundamental period lies between 0.1 and 0.6 s, thus, covering a wide range of values for possible earthquakes.

#### 3.2. The parameters $\kappa_1, \kappa_2$ , for typical soil slips

Figure 4 gives examples of typical soil slips for (a) an earth dam,<sup>4</sup> (b) rockfill dams,<sup>5</sup> (c) road and railway embankments near the sea,<sup>19</sup> and (d) natural slopes.<sup>2</sup> For the earthdam (Figure 4(a)), values of dam height of 8, 30 and 100 m are used, which are typical for dams with small, medium and large height, respectively. For the natural slopes, the slips correspond to the diagramatic failure cross-sections of slides in Maidiripo in China (Figure 4(d1)), in Catak in Turkey (Figure 4(d2)) and Usoi in China (Figure 4(d3)).<sup>2</sup> The model assumptions about non-existence of internal shearing and constant height hold only as approximations in the geometries of Figure 4.

Table I gives the estimates of the coefficients  $\kappa_1$  and  $\kappa_2$ , given by equations (6b) and (6c), for the soil slips of Figure 4. For height  $h$ , the average value of the heights is used in each location that the sliding mass changes inclination (shown with dotted lines in Figure 4). For strength and pore pressure, uniform conditions are assumed (i.e.  $\phi' = \phi'_i$ ,  $c' = c'_i$ ,  $R_u = R_{ui}$ ) and typical parameters are used for dry conditions ( $\phi' = 30^\circ$  and  $40^\circ$  with  $c' = 0$ ,  $R_u = 0$ ), saturated conditions in association with effective stress analysis ( $\phi' = 30^\circ$  and  $40^\circ$  with  $c' = 0$ ,  $R_u = 0.5$ ), and saturated conditions in association with total stress analysis ( $Su/\gamma h = c'/\gamma h = 0.5$  and 1 with  $\phi' = 0^\circ$ ,  $R_u = 0$ ). These typical parameters are selected, considering that dry conditions usually exist in sandy soils, where cohesion is small, and that for saturated conditions effective stress analysis is usually performed in sands, and total stress analysis in clays.<sup>16</sup> In association with total stress analysis, it is assumed that the undrained shear strength of clays,  $Su$ , is proportional to vertical stress, an assumption often made in soil mechanics.<sup>9,16</sup> An example of how  $\kappa_1$  and  $\kappa_2$  are calculated is given in Appendix II.

The slip length  $b_i$  is defined as the sum of the contact lengths in each inclination,  $b_i$ . It roughly represents the ratio  $\{A_i/h\}$ ; this is perfectly true if the sliding mass has constant height. Close inspection of equations (6b) and (6c) indicates that for given shape of geometry (i.e. given angles  $\theta_i$ ) and strength parameters (i.e. given  $\phi'_i$ ,  $c'_i/\gamma h$ ) the factors  $\kappa_1$  and  $\kappa_2$  are inversely proportional to the slip length  $b_i$ . Figure 5 plots the values of the factors  $\kappa_1$  and  $\{\kappa_2 g/\kappa_1\}$  for the geometries of Figure 4 in terms of the slip length and the soil parameters used. It can be observed that:

- (1) The factor  $\kappa_1$  is not affected considerably by the strength and pore pressure parameters along the surface of sliding. For slips of typical slopes, where the slip length is larger than 10 m, it takes values

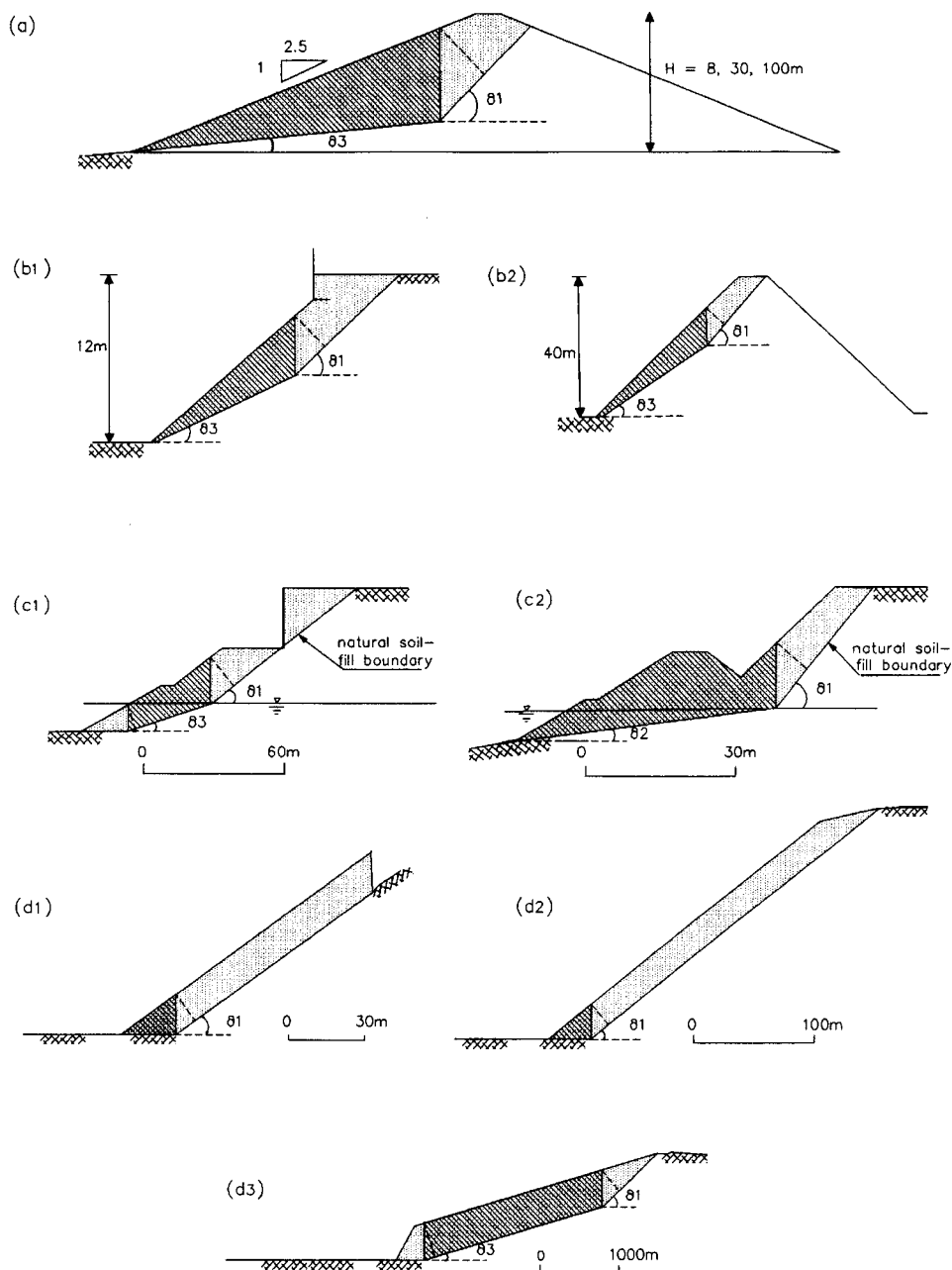


Figure 4. Typical sliding surfaces of (a) an earth dam;<sup>4</sup> (b1), (b2) rockfill dams;<sup>6</sup> (c1), (c2) embankments near the sea;<sup>19</sup> (d1)–(d3) natural slopes.<sup>2</sup> Shown is the division of the sliding mass according to the model of Figure 2. Note that for all cases, except for case (c2),  $\theta_2 = 0$

ranging between zero and  $1.5/s^2$ . Keeping the inverse proportionality between  $\kappa_1$  and  $b_t$ ,  $\kappa_1$  can be approximately related to the slip length as

$$\kappa_1 (\text{in } s^{-2}) = \frac{11}{b_t (\text{in m})} \quad (8)$$

- (2) The factor  $\kappa_2$ , similarly to  $\kappa_1$ , decreases with the slip length. For slips of typical slopes the ratio  $\{\kappa_2 g / \kappa_1\}$  does not exceed the value of about one.



Table I. The factors  $\kappa_1$  and  $\kappa_2$  for the geometries of Figure 4. Cases 1–6 correspond to strength and pore pressure parameters  $\{\varphi', c'/\gamma h, R_u\}$  equal to  $\{30^\circ, 0, 0\}$ ,  $\{40^\circ, 0, 0\}$ ,  $\{30^\circ, 0, 0.5\}$ ,  $\{40^\circ, 0, 0.5\}$ ,  $\{0^\circ, 0.5, 0\}$ ,  $\{0^\circ, 1, 0\}$ , respectively

	(a)										
	$H = 30 \text{ m}$	$H = 8 \text{ m}$	$H = 100 \text{ m}$	(b1)	(b2)	(c1)	(c2)	(d1)	(d2)	(d3)	
$b_1(\text{m})$	97	27	343	22	63	136	82	115	340	3660	
$h(\text{m})$	7	2	24	2	4	13	8	12	22	378	
$\theta_1(^{\circ})$	45	45	45	43	49	37	49	35	38	43	
$\theta_2(^{\circ})$	0	0	0	0	0	0	8	0	0	0	
$\theta_3(^{\circ})$	5	5	5	25	32	18	0	0	0	16	
$A_{10}(\text{m}^2)$	246	18	2733	25	128	714	162	1192	5961	158276	
$A_{20}(\text{m}^2)$	0	0	0	0	0	107	0	162	504	103781	
$A_{30}(\text{m}^2)$	697	49	7733	23	198	489	423	0	0	1030575	
$\kappa_1(\text{s}^{-2})$											
Case 1	0.069	0.26	0.021	0.34	0.13	0.079	0.11	0.073	0.030	0.0025	
Case 2	0.085	0.32	0.025	0.42	0.16	0.10	0.13	0.094	0.038	0.0031	
Case 3	0.064	0.24	0.019	0.31	0.11	0.078	0.091	0.072	0.029	0.0023	
Case 4	0.088	0.33	0.026	0.44	0.16	0.11	0.11	0.10	0.041	0.0033	
Case 5	0.10	0.36	0.030	0.46	0.20	0.10	0.18	0.086	0.037	0.0034	
Case 6	0.11	0.43	0.034	0.53	0.23	0.11	0.22	0.10	0.043	0.0040	
$\kappa_2(\text{m}^{-1})$	0.0050	0.018	0.0014	0.022	0.010	0.0045	0.010	0.0039	0.0017	0.00017	

Geometry (see Figure 4)

$$\{\phi', c'/\gamma h, R_u\}: \quad \square \{30^\circ, 0, 0\} \quad + \{40^\circ, 0, 0\} \quad \diamond \{30^\circ, 0, 0.5\} \\ \triangle \{40^\circ, 0, 0.5\} \quad \times \{0^\circ, 0.5, 0\} \quad \circ \{0^\circ, 1, 0\}$$

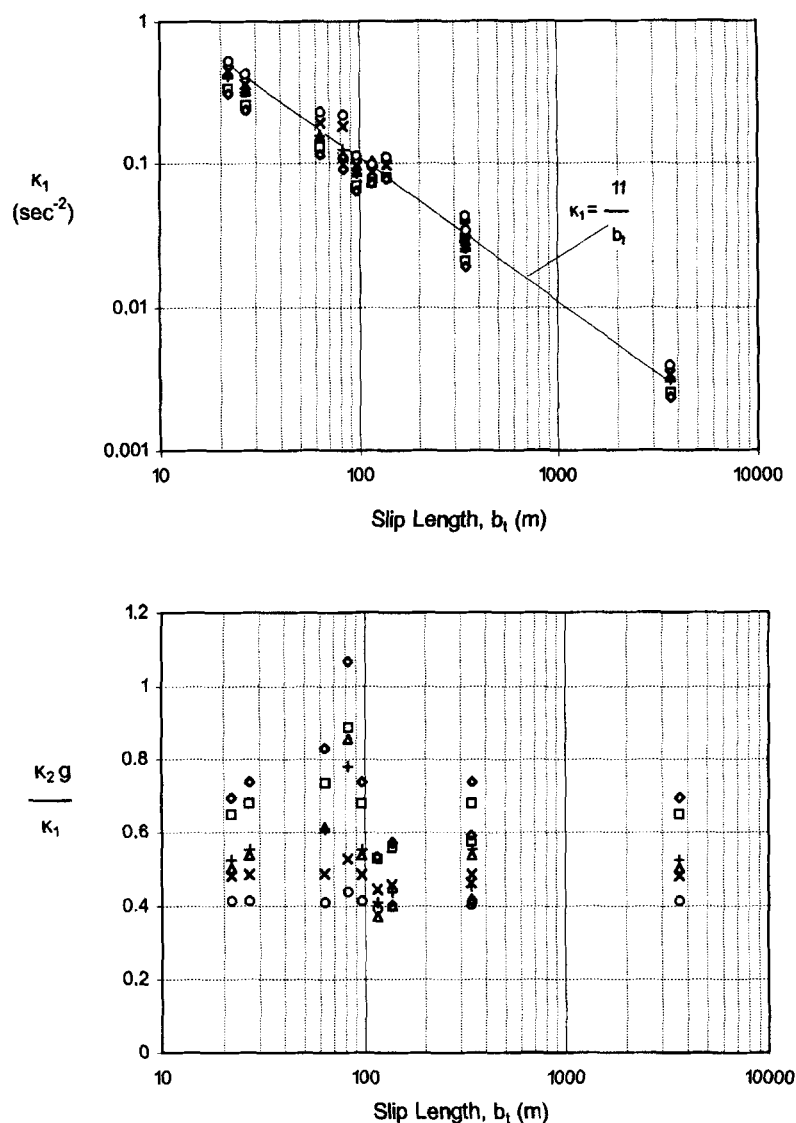


Figure 5. The factors  $\kappa_1$  and  $(\kappa_2 g / \kappa_1)$  in terms of the slip length for the geometries of Figure 4

### 3.3. Approximation of equation (7)

According to the previous section, for typical slopes, the slip length does not exceed 10 m, the factor  $\kappa_1$  can be related to the slip length using equation (8), and the factor  $\{\kappa_2 g / \kappa_1\}$  does not exceed the value of one. Figure 6 compares the numerical solution of equation (7) for (a)  $\kappa_2 = \kappa_1 / g$  and (b)  $\kappa_2 = 0$  for the accelerograms described in Section 3.1 in terms of the slip length and the acceleration ratio  $a_{c0} / a_m$ . Equation (8) is used to relate the slip length to  $\kappa_1$ . The difference in results is less than 1.2 per cent.

From the above it is concluded that for earthquake slips of typical slopes the dimensionless factor  $\{2 / (1 + (1 + S\kappa_2)^{0.5})\}$  of equation (7) takes values very close to unity, and equation (7) can be

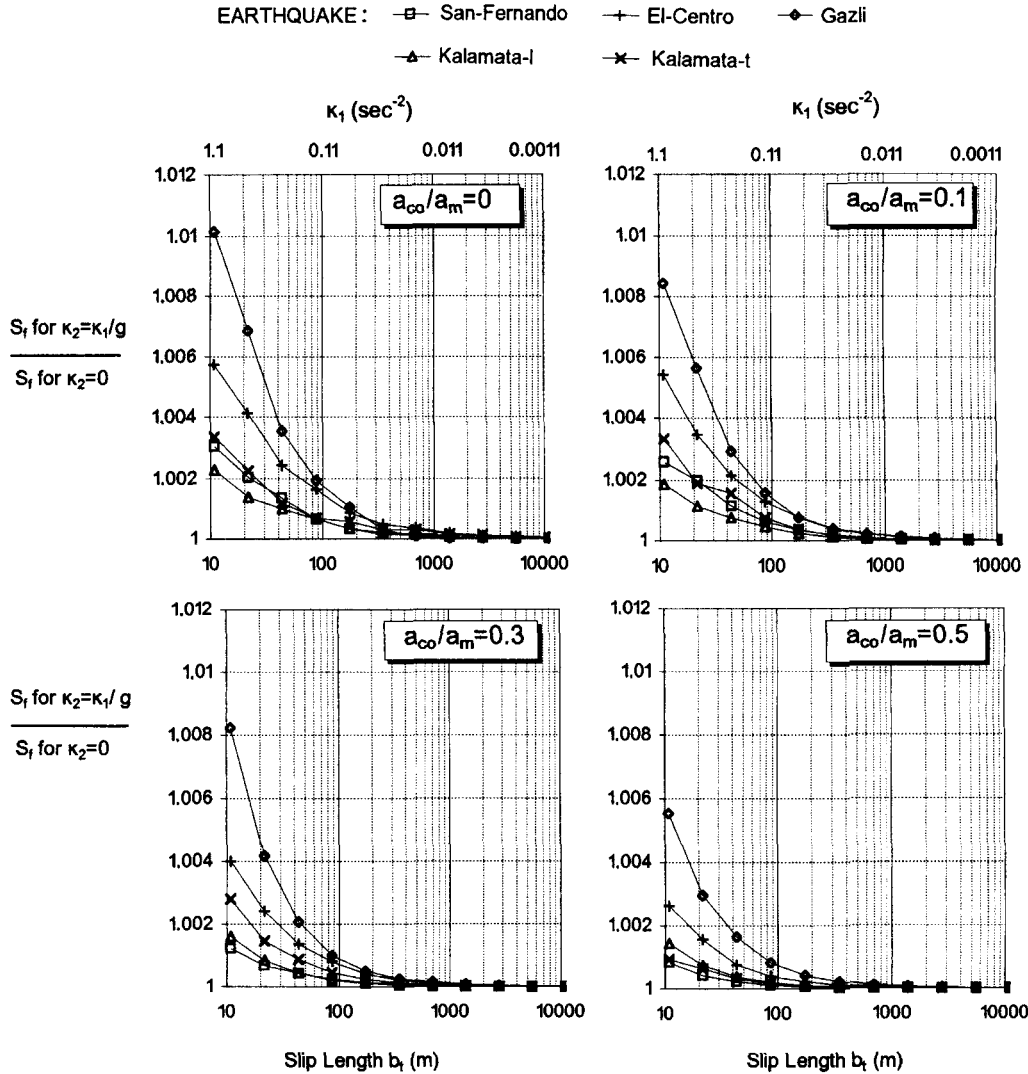


Figure 6. Comparison between the total displacement that equation (9) predicts when  $\kappa_2 = \kappa_1/g$  and when  $\kappa_2 = 0$ , in terms of the slip length, the acceleration ratio and the applied accelerogram

approximated as

$$\frac{d^2S}{dt^2} = a(t) - a_{c0} - S\kappa_1 \quad \text{for } dS/dt > 0 \quad (9)$$

It can be noted that equation (7) for  $\kappa_2 = 0$  gives equation (9) and thus the computer program, discussed earlier, that solves equation (7), can also solve equation (9).

#### 4. SOLUTION IN COMPARISON TO THE SLIDING BLOCK MODEL

##### 4.1. Solutions of the sliding-block model

In the sliding-block model of Figure 1, the motion of the block on the inclined plane can be described as

$$\frac{d^2S}{dt^2} = a(t) - a_{c0} \quad \text{for } dS/dt > 0 \quad (10)$$

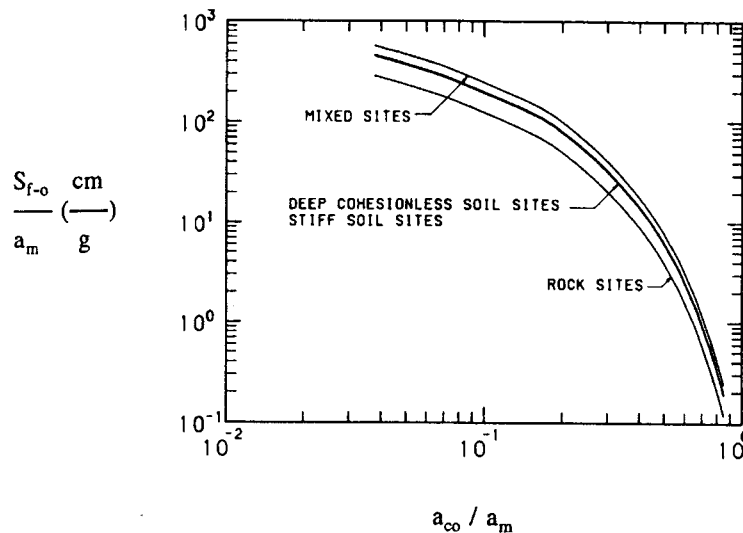


Figure 7. Permanent seismic displacement of the sliding-block model<sup>20</sup>

where  $S$  is the horizontal distance moved,  $a_{c0}$  is the (constant and initial) critical acceleration for which relative motion develops and  $a(t)$  is the applied horizontal accelerogram. The solution giving the distance moved by the block depends on characteristics of the applied earthquake. For example, Lin and Whitman<sup>20</sup> give analytical solutions of the horizontal distance moved by the block,  $S_{f-0}$ , for sinusoidal, rectangular and triangular excitations. In addition, for seismic excitations they use statistical methods to obtain the distance that the block moves in terms of the maximum applied horizontal acceleration, the critical acceleration and the site type (Figure 7).

It can be noted that for the accelerograms that are applied in the present work, described in Section 3.1, the displacements of the sliding-block model,  $S_{f-0}$ , were estimated by solving numerically equation (10) for various acceleration ratios  $a_{c0}/a_m$ . The relationships of the distance moved divided by the maximum applied acceleration,  $S_{f-0}/a_m$ , in terms of the acceleration ratio  $a_{c0}/a_m$ , were found not to vary considerably from earthquake to earthquake and to be in the small band of the relationships recommended by Figure 7.<sup>21</sup>

#### 4.2. Solutions of equation (9)

The difference of equation (9) that describes approximately the motion of the new sliding system of Figure 2, from equation (10) of the sliding-block model is the term  $\{-S\kappa_1\}$ . To illustrate this, it can be stated that, if the sliding-block model was used to approximate the dynamic motion of the new sliding system, equation (10) would have been used, with the critical acceleration  $a_{c0}$  estimated by equation (5).

The solution of equation (9) will be presented as the dimensionless distance  $S_f/S_{f-0}$ , where  $S_f$  is the horizontal distance that the centre of mass of the chain of Figure 2 moves as a result of its downward slip, and  $S_{f-0}$  is the corresponding distance for  $\kappa_1 = 0$ , that is equivalent to the distance moved by the sliding-block model for similar initial critical acceleration and applied excitation. This dimensionless distance will be related to (a) the coefficient  $\kappa_1$ , or the equivalent slip length according to equation (8), and (b) the ratio of the initial critical acceleration by the maximum applied acceleration  $a_{c0}/a_m$ . Based on equation (9), these relationships can depend on characteristics of the applied excitation such as its fundamental period, time duration and number of loading/unloading cycles.

When rectangular, triangular and sinusoidal harmonic excitations were applied in equation (9) the following were observed:

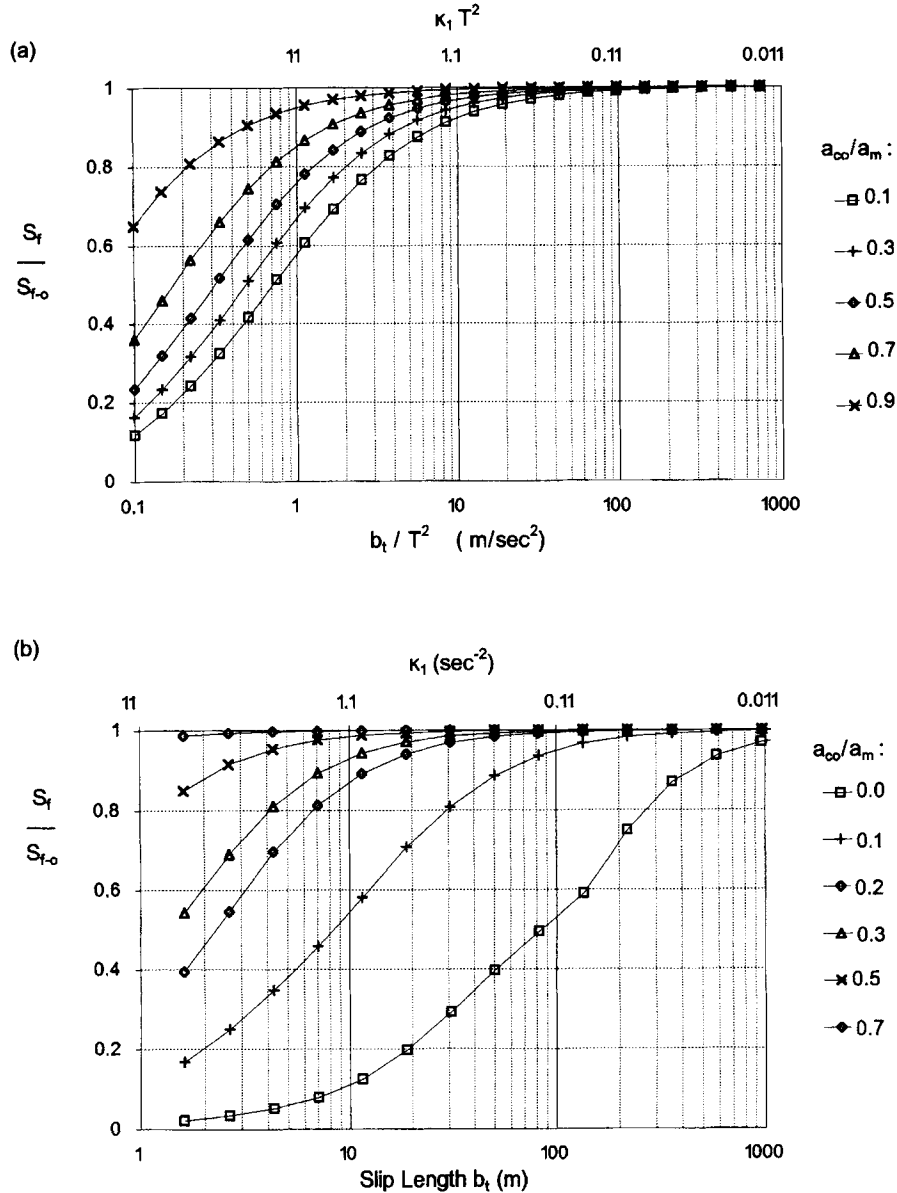


Figure 8. Permanent displacement of the new model, normalized by that of the sliding-block model for similar initial critical acceleration and applied excitation for (a) one cycle of sinusoidal excitation with period  $T$ , (b) the earthquake of San-Fernando

- (i) The ratio  $S_f/S_{f-0}$  decreases from one to zero as the factor  $\kappa_1$  increases from zero, or equivalently as the slip length  $b_t$  decreases. For a given value of the factor  $\kappa_1$ , the ratio  $S_f/S_{f-0}$  decreases as the ratio  $a_{c0}/a_m$  decreases. Figure 8(a) gives the results for one cycle of sinusoidal excitation.
- (ii) The maximum applied acceleration does not affect the above relationships.
- (iii) The period of the excitation  $T$  does not affect the above relationships if the factor  $\kappa_1$  is replaced by the factor  $\{\kappa_1 T^2\}$ .
- (iv) The effect of the number of cycles of unloading-reloading,  $N$ , can be approximated by replacing the factor  $\{\kappa_1 T^2\}$  with the factor  $\{\kappa_1 T^2 N\}$ . The above relationship is exact for  $\kappa_1$  zero and its accuracy decreases as  $\kappa_1$  increases.

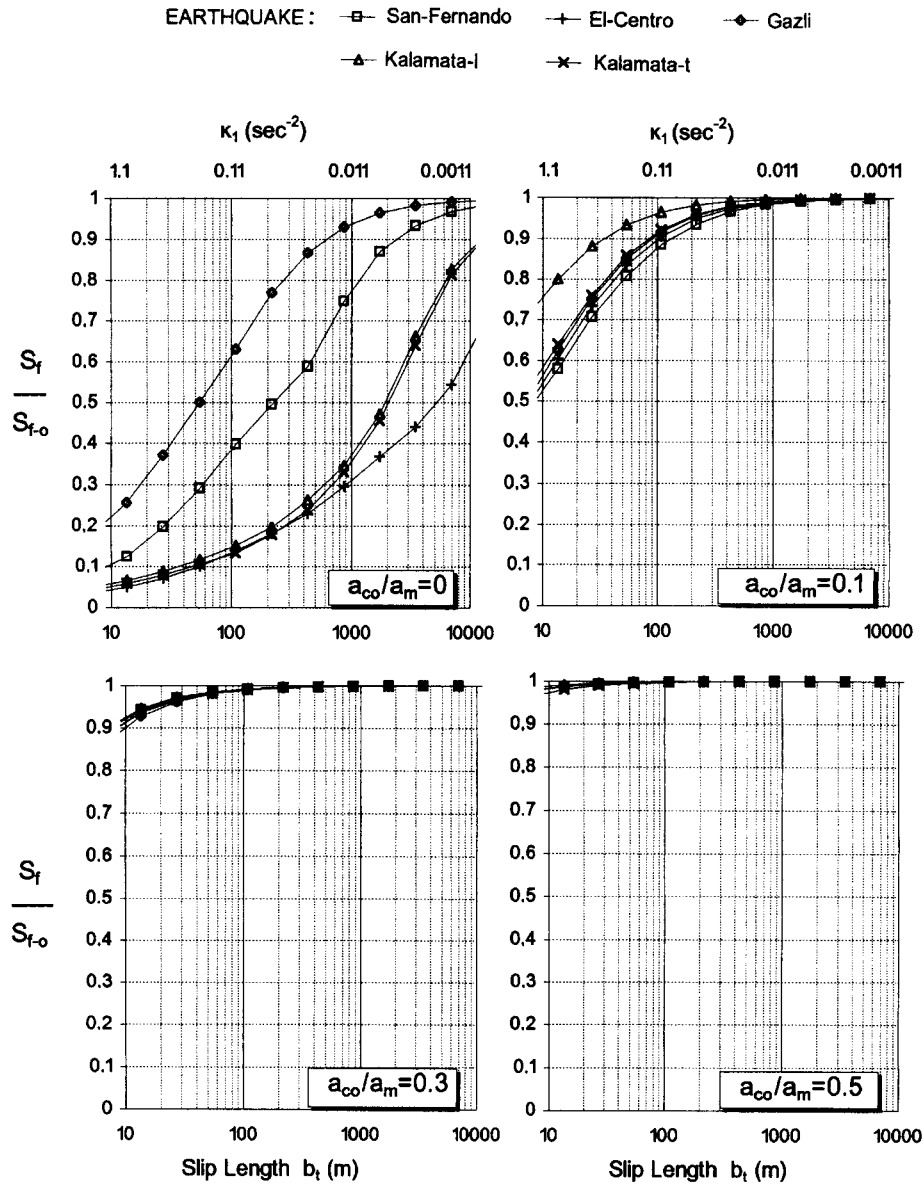


Figure 9. Permanent displacement of the new model normalized by that of the sliding-block model for similar initial critical acceleration and applied excitation, in terms of the slip length, the acceleration ratio and the applied accelerogram

- (v) Rectangular harmonic excitations of equal maximum acceleration and period give a larger decrease of the ratio  $S_f/S_{f-0}$  and triangular excitations a smaller decrease in comparison to the sinusoidal excitations.
- (vi) As the factor  $\kappa_1$  is inversely proportional to the slip length, in the above relationships the factors  $\{\kappa_1 T^2\}$  and  $\{\kappa_1 T^2 N\}$  can also be expressed by the factors  $\{b_t/T^2\}$  and  $\{b_t/(T^2 N)\}$ .

Solutions for earthquake excitations are of more practical interest because they represent what occurs in the field. Figure 9 gives the numerical solutions of equation (9) for the five (5) accelerograms described in Section 3.1. It is observed that for given acceleration ratio  $a_{c0}/a_m$  and  $\kappa_1$ , the effect of the applied accelerogram in the ratio  $S_f/S_{f-0}$  is small, especially for acceleration ratios greater than, or equal to 0.3. Figure 8(b) gives the results of the San-Fernando earthquake in more detail.

#### 4.3. Discussion — results for typical slips of slopes

The difference between equation (9), that approximately describes the motion of the new model, and the equation of motion of the block-on-an-inclined-plane model is the term  $\{-S\kappa_1\}$ , where the factor  $\kappa_1$  is approximately inversely proportional to the slip length. The following can be concluded that agree with the results of the numerical analyses:

- (a) For given excitation and critical acceleration  $a_{c0}$ , an increase of the factor  $\kappa_1$ , or decrease of the slip length, increases the difference between the distance moved by the two models.
- (b) For given  $\kappa_1$  and shape of excitation, the difference in the distance moved by the two models increases with a decrease of the critical acceleration  $a_{c0}$  and an increase of the maximum applied acceleration  $a_m$ , because the distance moved  $S_f$  increases. However, a constant acceleration ratio  $a_{c0}/a_m$  gives a constant displacement ratio  $S_f/S_{f-0}$ .
- (c) For given coefficient  $\kappa_1$ , critical acceleration  $a_{c0}$ , and maximum applied acceleration  $a_m$  of harmonic excitation, the difference in predictions of the two models increases as the period, the number of cycles of loading/unloading and the area of the loop of the harmonic excitation increase. This is again due to the increase of the displacement  $S_f$ .

Figure 8(b) shows that for ratios  $a_{c0}/a_m$  equal to 0.0, 0.1, 0.2 and 0.3, the numerical results give values of the ratio  $S_f/S_{f-0}$ , for a slip length of 100 m ( $\kappa_1 = 0.11/s^2$ ) equal to 0.5, 0.9, 1 and 1, while for a slip length of 10 m ( $\kappa_1 = 1.1/s^2$ ) equal to 0.1, 0.5, 0.85 and 0.9, respectively. Thus, the change in the predictions of permanent seismic movement of the new model of Figure 2, in comparison to that of Newmark's sliding-block model of Figure 1, can be significant only when the ratio of accelerations  $a_{c0}/a_m$  takes values smaller than about 0.2.

The ratio  $a_{c0}/a_m$  takes values smaller than 0.2 for sliding surfaces with a static factor of safety not much larger than one, either initially, or as a result of earthquake-induced decrease in strength. Specifically, excluding soil amplification along the height of the slope, for earthquakes with Richter magnitude up to 7, and distances of more than 5 km from the epicenter, the maximum acceleration  $a_m$  cannot exceed the value of about  $0.5g$ .<sup>22</sup> In earth dams and embankments the critical acceleration  $a_{c0}$  takes values smaller than  $0.1g$ , and thus the acceleration ratio  $a_{c0}/a_m$  is smaller than 0.2, at sliding surfaces with a static factor of safety smaller than about 1.4.<sup>23</sup> It can be noted that for such small acceleration ratios, for typical earthquakes, seismic displacements are large, i.e. larger than about 0.3 m, as indicated by Figure 7.

## 5. DISCUSSION

### 5.1. Improved method predicting co-seismic deformations

As already illustrated, the change in the predictions of permanent seismic movement of the new sliding system of Figure 2, in comparison to that of Newmark's sliding-block model, is significant when earthquake-induced soil slips have an anticipated ratio of accelerations  $a_{c0}/a_m$  less than about 0.2. For soil slips with this characteristic it is suggested to use the new sliding system of Figure 2 for the prediction of permanent co-seismic deformations using the procedure outlined below.

The critical sliding surface for the earth mass under consideration, and its initial critical acceleration  $a_{c0}$ , can be estimated by stability analysis, similarly to the applications of the sliding-block model. To be consistent with the model of Figure 2, it is recommended to use stability analysis assuming a sliding surface consisting of linear segments,<sup>17</sup> and not circular. For dry soil, stability analyses should be performed using the friction and cohesion components of strength. For saturated soil, it is recommended to use analysis in terms of total stresses for clays, and analysis in terms of effective stresses for sandy soils. When total stress analysis is performed, the undrained shear strength of the soil should be used, and the frictional component of the resistance should be taken zero. When effective stress analysis is performed, the effective strength parameters and pre-seismic pore pressures should be used, and pore-pressure build-up during the loading part of dynamic cycles should be taken into account.<sup>4</sup>

Earthquake-caused degradation in strength must be considered, when anticipated. Such degradation can occur in saturated soils.<sup>4,5,9</sup> In association with total stress analysis, it can be taken into account, conservatively, by using the 'fast residual'<sup>9</sup> instead of the 'peak' undrained shear strength of the soil, when estimating,  $a_{c0}$ . In association with effective stress analysis, it can be taken into account, conservatively, by adding to pre-seismic pore-pressures end-of-shaking anticipated pore-pressure build-up, when estimating,  $a_{c0}$ . These may produce negative values of  $a_{c0}$ , e.g. when the residual soil strength is less than the shear strength required for equilibrium.

The maximum applied seismic acceleration at the bedrock is usually obtained from results of analyses of seismic hazard at the site of interest. For better predictions, amplification of acceleration along the height of the slope should be considered when estimating the maximum acceleration on the surface of sliding,  $a_m$ , similarly to applications of the sliding-block model.<sup>4,5</sup>

Having estimated the critical sliding surface,  $a_{c0}$  and  $a_m$ , permanent seismic deformations should be obtained either by solving equation (7) for the design accelerograms of the slope of interest, or by correcting (decreasing) predictions of the sliding-block model<sup>20</sup> in terms of the anticipated ratio of accelerations  $a_{c0}/a_m$ , using Figure 8(b). Figure 8(b) can be used either in terms of the slope slip length, or more accurately in terms of the coefficient  $\kappa_1$ . It should be used in terms of the slip length only for slips of slopes with geometries similar to those considered in Figure 4. Use of Figure 8(b) is not appropriate when the ratio  $a_{c0}/a_m$  takes values equal to or less than zero, as the results depend on details of the applied accelerogram (Figure 9). When seismic deformations are estimated using the factor  $\kappa_1$  or equation (7), the factors  $\kappa_1$  and  $\kappa_2$  of the critical sliding surface should be obtained using equations (6b) and (6c), as described in Section 3.2, and illustrated in Appendix II.

### 5.2. Potential application of the new sliding system

In the paper, the derivations assumed constant soil strength and pore pressure during the duration of dynamic loading. To formulate a more accurate simplified method predicting permanent seismic shear deformations for soils with earthquake-caused changes in strength, methods modelling such decreases can be used in association with the new sliding system of Figure 2. Results will depend, in the case of total stress analysis on strain-dependent shear strength,<sup>9</sup> and in the case of effective stress analysis on progressive earthquake-induced excess pore pressure build-up.<sup>10</sup>

With this method, post-seismic displacements, that will develop if, e.g., the 'fast residual' shear strength of the soil is less than the shear strength required for static equilibrium, can also be predicted. This can be accomplished by extending the numerical integration of equation (7) after the application of the seismic excitation  $a(t)$ , until the velocity  $dS/dt$  becomes zero. This is in contrast to the current sliding-block model that overpredicts post-seismic displacements, since when the static factor of safety of a block-on-an-inclined-plane is less than one, infinite movement of the block develops.

## 6. CONCLUSIONS

The current sliding-block model is widely used for the prediction of permanent co-seismic ground deformations related to shearing. It represents motion of an infinite slope and does not take into account the possible change in inclination of the sliding earth mass, as a result of its movement. For the investigation of this effect the present paper studies the dynamic motion of a perfectly flexible chain sliding downwards in ' $n$ ' planes with gradually decreasing inclinations. To simplify the problem it is assumed that the part of the chain that changes inclinations has uniform height (Figure 2).

The approximate governing equation of motion of the new sliding system was formulated (Equation (7)). It was shown that for slips of typical slopes the parameters take such values that this equation can be approximated by equation (9). Equation (9) differs from the governing equation of the sliding-block model by the factor  $\{-\kappa_1 S\}$ , where the coefficient  $\kappa_1$  is approximately inversely proportional to the slip length, and  $S$  is the permanent horizontal distance moved by the centre of mass of the sliding body. Numerical solutions of equation (9) for various earthquakes illustrated that the difference in the predictions of the new model from



those of the widely used sliding-block model for similar initial critical acceleration and applied excitation is small, except where the ratio of the critical acceleration by the maximum applied acceleration  $a_{c0}/a_m$  takes values smaller than about 0.2. The difference in predictions increases as the slip length decreases.

For soil slips with acceleration ratios  $a_{c0}/a_m$  less than 0.2, it is recommended to use the sliding system of Figure 2. Permanent deformations can be estimated, either by solving equation (7) using the appropriate parameters of the sliding mass under consideration and design accelerogram, or by reducing the predictions of the sliding-block model in terms of the slope slip length and the acceleration ratio  $a_{c0}/a_m$  using the relationships of Figure 8(b).

#### ACKNOWLEDGEMENTS

This work was funded by the Hellenic Organization of Aseismic Design and Protection (O.A.S.P.) in 1993 and 1994. Aris Stamatopoulos made valuable suggestions. Argyris Alexandris assisted in the selection of the applied accelerograms. Lidia Balla drafted the figures.

#### NOTATION (Partial List)

$A_i, h, b_i, \theta_i$	parameters that define the geometry of the 'chain' of Figure 2
$A_{i0}, b_{i0}$	initial values of the parameters $A_i, b_i$ (when $u = S = 0$ )
$A_t, b_t$	total values of the area and slip length of the 'chain' of Figure 2
$a(t)$	acceleration of the applied excitation in terms of time
$a_c$	critical acceleration, i.e. the horizontal acceleration that causes sliding
$a_{c0}$	critical acceleration of the body of Figure 1, or of the body of Figure 2 when $u = S = 0$
$a_m$	maximum acceleration of the applied excitation
$c'_i, \phi'_i$	effective cohesion and friction angle on the surface of sliding with inclination $\theta_i$
$d$	differential
$g$	acceleration of gravity
$K, \kappa_1, \kappa_2$	factors given by equations (6a)–(6c)
$i$	pointer of a slice of the sliding mass (Figure 2)
$N$	number of cycles of loading-unloading
$R_{ui}$	ratio of pore pressure by total vertical stress on the surface of sliding with inclination $\theta_i$
$S$	horizontal distance moved by the center of mass of the sliding body, as a result of its downward movement $u$
$S_f$	total distance $S$ moved by the sliding body
$S_{f-0}$	$S_f$ of the system of Figure 1, or of Figure 2 for $\kappa_1 = 0$
$t$	time
$T$	period of harmonic excitation
$u$	downward distance moved by the body of Figure 2 along the surface of sliding

#### APPENDIX I

##### *Solution of equation (3a)*

We solve the following equation:

$$dS = \frac{\sum_{i=1}^n (A_{i0} \cos \theta_i) + uh(\cos \theta_2 - \cos \theta_1)}{A_t} du \quad (11)$$

Integration of both sides gives

$$S = u \frac{\sum_{i=1}^n (A_{i0} \cos \theta_i) + 0.5uh(\cos \theta_2 - \cos \theta_1)}{A_t} \quad (12a)$$

or that

$$u^2(0.5 h(\cos \theta_2 - \cos \theta_1)) + u \sum_{i=1}^n (A_{i0} \cos \theta_i) - SA_t = 0 \quad (12b)$$

Solution for 'u' gives

$$u = \frac{-\sum_{i=1}^n A_{i0} \cos \theta_i + ((\sum_{i=1}^n A_{i0} \cos \theta_i)^2 + 2Sh(\cos \theta_2 - \cos \theta_1) A_t)^{0.5}}{h(\cos \theta_2 - \cos \theta_1)} \quad (13a)$$

Equation (12a) can be expressed as

$$u = \frac{SA_t}{\sum_{i=1}^n (A_{i0} \cos \theta_i) + 0.5uh(\cos \theta_2 - \cos \theta_1)} = \frac{SA_t / \sum_{i=1}^n (A_{i0} \cos \theta_i)}{1 + 0.5uh(\cos \theta_2 - \cos \theta_1) / \sum_{i=1}^n (A_{i0} \cos \theta_i)} \quad (12c)$$

In addition, equation (13a) can be expressed as

$$\frac{uh(\cos \theta_2 - \cos \theta_1)}{\sum_{i=1}^n (A_{i0} \cos \theta_i)} = -1 + \left(1 + \frac{2Sh(\cos \theta_2 - \cos \theta_1) A_t}{(\sum_{i=1}^n A_{i0} \cos \theta_i)^2}\right)^{0.5} \quad (13b)$$

Finally, equations (12c) and (13b) give

$$u = \frac{2SA_t / \sum_{i=1}^n (A_{i0} \cos \theta_i)}{1 + \left(1 + \frac{2Sh(\cos \theta_2 - \cos \theta_1) A_t}{(\sum_{i=1}^n A_{i0} \cos \theta_i)^2}\right)^{0.5}} \quad (14)$$

## APPENDIX II

*Example of calculating the factors  $\kappa_1, \kappa_2$*

The geometry of Figure 4a is considered, for the case of a dam height,  $H$ , equal to 30 m and a frictional resistance of  $30^\circ$ . Cohesion and pore pressure are taken zero. Sliding occurs in three inclinations with:

$$\theta_1 = 45^\circ, \quad A_{10} = 246 \text{ m}^2$$

$$\theta_2 = 0^\circ, \quad A_{20} = 0$$

$$\theta_3 = 5^\circ, \quad A_{30} = 690 \text{ m}^2$$

For height  $h$ , the average value of the heights in each location that the sliding mass changes inclination (between inclination 1–3 and 3–2) is used:  $h = (h_{1-3} + h_{3-2})/2 = (14 + 0)/2 = 7 \text{ m}$ . The above values of angles, areas and length were estimated using CAD software.

For these values, equations (6b) and (6c) give

$$\kappa_1 = g(\tan(\varphi' - \theta_2) - \tan(\varphi' - \theta_1)) \frac{h}{\sum_{i=1}^n (A_{i0} \cos \theta_i)} = 9.81 \times 0.86 \times 0.0082 = 0.069/\text{s}^2$$

$$\kappa_2 = 2(\cos \theta_2 - \cos \theta_1) \frac{h A_t}{(\sum_{i=1}^n A_{i0} \cos \theta_i)^2} = 2 \times 0.29 \times 0.0082 = 0.0048/\text{m}$$

## REFERENCES

1. R. V. Whitman, 'Predicting earthquake-caused permanent deformations of earth structures', article on '*Predictive Soil Mechanics*', Thomas Telford, London, pp. 729–741 (1993).
2. N. N. Ambraseys and M. Srbulov, 'Earthquake induced displacements of slopes', *Soil dyn. earthquake Eng.* **14**, 59–71 (1995).
3. N. M. Nemark, 'Effect of earthquakes on dams and embankments', *Geotechnique* **15**, 139–160 (1965).
4. S. K. Sarma, 'Seismic stability of earth dams and embankments', *Geotechnique* **25**, 743–761 (1975).
5. F. I. Makdisi and H. B. Seed, 'Simplified procedure for estimating dam and embankment earthquake-induced deformations', *ASCE proc. j. geotech. eng. div.* **104**, 849–867 (1978).
6. G. Gazetas and P. Dakoulas, 'Seismic analysis and design of rockfill dams: state-of-the-art', *Soil dyn. earthquake eng. j.* **11**, 27–61 (1992).

7. R. Richards Jr. and D. Elms, 'Seismic behavior of gravity retaining walls', *ASCE proc. j. geotech. eng. div.* **105**, 449–464 (1979).
8. R. Richards Jr., D. Elms and M. Budhu, 'Seismic bearing capacity and settlements of foundations', *ASCE proc. j. geotech. eng. div.* **119**, 662–674 (1993).
9. Th. Tika-Vassilikos, S. Sarma and N. N. Ambraseys, 'Seismic displacements on shear surfaces on cohesive soils', *Earthquake eng. struct. dyn.* **22**, 709–721 (1993).
10. H. Modaressi, D. Aubry, E. Faccioli and C. Noret, 'Numerical modelling approaches for the analysis of earthquake triggered landslides', *3rd int. conf. on recent advances in geotechnical earthquake*, St. Louis, Vol. 2, pp. 833–843 (1995).
11. S. K. Sarma, 'Seismic displacement analysis of earth dams', *ASCE proc. j. geotech. eng. div.* **107**, 1735–1739 (1981).
12. L. Lemos, A. Gama and P. Goelho, 'Displacement of cohesive slopes induced by earthquake loading', *Proc. int. conf. soil mech. & found. eng.*, Vol. 3, New Delhi, pp. 1041–1045 (1994).
13. C. Stamatopoulos, 'Analysis of a slide parallel to the slope', *Proc. 2nd Greek natl. conf. geotech. engng*, Vol. 1, pp. 481–488 (1992) (in Greek).
14. C. Stamatopoulos, 'Prediction of permanent movement of triangular slides after soil liquefaction', *Earthquake Resistant Construction and Design*, *Proc. 2nd int. conf. on earthquake resistant construction and design*, A. A. Balkema, Rotterdam, Vol. 1, pp. 243–250 (1994).
15. S. Timoshenko, D. H. Young, *Advanced Dynamics*, McGraw-Hill Company, New York, Article 19, 1948.
16. T. W. Lambe and R. V. Whitman, 'soil mechanics', Wiley, New York, Chapters 11, 29, 30, 1969.
17. S. K. Sarma, 'Stability analysis of embankments and slopes', *Geotechnique* **23**, 423–433 (1973).
18. G. Dahlquist, A. Björck and N. Anderson (translator), 'Numerical Methods', Prentice-Hall, Englewood Cliffs, NJ, Section 8.2, 1974.
19. E. Stara-Gazeta and G. Gazetas, 'Seismic stability of twin embankments of the rail-highway crossing of Megara Bay', *Proc. 2nd Greek natl. conf. geotech. engng*, Vol. 2, pp. 289–296 (1992) (in Greek).
20. J. S. Lin and R. V. Whitman, 'Earthquake induced displacements of sliding blocks', *J. geotech. eng. ASCE proc.* **112**, 44–59 (1986).
21. C. Stamatopoulos, Research titled 'Formulation of theoretical relationships for the prediction of seismic movements of slopes', *3rd (and final) Report to O.A.S.P.*, 1994 (in Greek).
22. N. N. Ambraseys and J. J. Bommer, 'The attenuation of ground accelerations in Europe', *Earthquake eng. struct. dyn.* **20**, 1179–1202 (1991).
23. S. K. Sarma and M. V. Bhawe, 'Critical acceleration versus static factor of safety in stability analysis of earth dams and embankments', *Geotechnique* **24**, 661–665 (1974).